Results in Surfaces and Interfaces 6 (2022) 100032

Contents lists available at ScienceDirect

Results in Surfaces and Interfaces

journal homepage: www.elsevier.com/locate/rsurfi

Analysis induced reduction of a polyelectrolyte

Rachel L. McLaren [a], Gareth R. Owen [a], David J. Morgan [b,c,*]

[a] School of Applied Science, University of South Wales, Treforest, CF37 4AT, UK
[b] Cardiff Catalysis Institute, School of Chemistry, Cardiff University, Cardiff, CF10 3AT, UK
[c] Harwell XPS, EPSRC National Research Facility for X-ray Photoelectron Spectroscopy, Didcot, Oxon, OX11 0FA, UK

ABSTRACT

The polymer, poly(diallyldimethylammonium chloride) (PDDA), is shown to undergo chemical change *via* a reduction mechanism during X-ray analysis. Examination of the N 1s spectrum of PDDA shows a time dependence on the degree of reduction, together with clear amplification of the extent of reduction through the charge compensation system and X-ray irradiation.

1. Introduction

X-ray Photoelectron Spectroscopy (XPS) is a well-established, valuable tool for the analysis of the elemental and chemical composition of a surface. In such analysis, the sample is irradiated with X-rays (commonly with a photon energy below 1.5 keV), resulting in a cascade of ejected photoelectrons, each with a kinetic energy which can be related to its binding energy and therefore representative of the orbital from which the electron was emitted (Stevie and Donley, 2020). Whilst routine XPS analysis is typically considered non-destructive, many materials have been shown to undergo damage (Stevie and Donley, 2020; Crist, 2000; Beamson and Briggs, 1992). Such damage can be initiated by the incident X-ray photons, secondary electron emission from the sample or thermal effects from the use of a non-monochromatic X-ray source, with polymers, ionic compounds, thin films and self-assembled monolayers (SAMs) amongst some of the materials known to undergo changes during XPS analysis (Wagner et al., 2000; Mendes et al., 2003; Cazaux, 1999; Baer et al., 2003a; Greczynski and Hultman, 2021; Rieke et al., 1993; Heister et al., 2001; Frydman et al., 1997; Moon et al., 1998; La et al., 2002b,a; Laibinis et al., 1991; Zharnikov and Grunze, 2002; Cazaux, 2000) These changes may result in significant changes to the core-level spectra, such as peak broadening, alterations to elemental composition and functional groups and loss of aromaticity as evidenced by the loss of satellite structure (Baer et al., 2003a). A well-known example undergoing such analysis-induced changes is polyvinylchloride (PVC), which has been shown to lose chlorine with increasing analysis time, causing significant change in the carbon spectra (Beamson and Briggs, 1992; Baer et al., 2003b). Ultimately, the effect of analysis induced damage is not just limited to the sample but can also lead to inaccurate conclusions being drawn based on the recorded spectra, and whilst an ISO standard for assessing analysis induced damage to a sample exists (ISO 18554:2016), it is not generally referenced by many analysts. Recognising whether a material is susceptible to sample damage, and thus taking steps to avoid it, is paramount towards obtaining accurate elemental composition data (Baer et al., 2003a). Herein, we report for the first time, the observed analysis induced modification of poly(diallyldimethylammonium chloride) (PDDA), a widely used polyelectrolyte for application within waste water treatment and membrane technology (McLaren et al., 2021a; Kam and Gregory, 1999). In particular, PDDA has been shown to aid the formation of carbon thin films utilising a porous plasma-exfoliated graphitic material (McLaren et al., 2021a,b, 2020). We investigate the changes to the polyelectrolyte by primarily focusing on the N 1s spectrum in detail, as well as investigating the effect of both the X-ray source and neutraliser as potential causes for the chemical modification of the polyelectrolyte.

2. Experimental

All work was performed using a Thermo Scientific K-Alpha$^+$ photoelectron spectrometer, which utilises a micro-focused monochromatic Al source (photon energy 1486.6 eV) operating at 6 mA x 12 kV (72 W). All data was recorded using the 400 μm spot mode, which has an elliptical area of approximately 400 × 600 μm^2. Charge compensation in the system is performed using a combination of low energy electrons and low energy argon ion to obtain a neutral and stable surface potential for analysis, under these conditions the C(1s) binding energy of the C–C bond in polyethylene terephthalate (PET) is found to be 284.8 eV.

For the degradation studies, the following protocols were used:

1. For conventional analysis, a full set of high-resolution core-level spectra were recorded quickly before iteratively collecting N 1s spectra from the same spot. Here the sample was constantly irradiated by both X-ray spot and neutraliser for a total time of *ca.* 70 min. Finally, the core-level spectra were recorded again.

* Corresponding author at: Cardiff Catalysis Institute, School of Chemistry, Cardiff University, Cardiff, CF10 3AT, UK.
E-mail address: MorganDJ3@cardiff.ac.uk (D.J. Morgan).

https://doi.org/10.1016/j.rsurfi.2021.100032
Received 7 October 2021; Received in revised form 15 November 2021; Accepted 22 November 2021

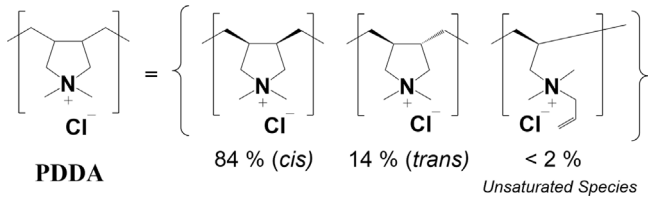

Fig. 1. Monomeric components of PDDA consisting of the *cis* and *trans* isomers and an unsaturated impurity.

Table 1
Quantitative elemental data for PDDA acquired at 0 min (T_0) and 70 min (T_{70}) intervals.

Element and orbital	Relative atomic concentration (%)	
	T_0	T_{70}
C 1s	70.5	71.0
N 1s	6.6	7.5
O 1s	10.0	9.0
Cl 2p	7.7	6.6
Na 1s	3.1	3.8
S 2p	2.1	2.1

The total acquisition time for the core-level and survey spectra was <5 min.

2. To investigate the effect of the X-rays, the high-resolution spectra were acquired as in (1). The neutraliser was subsequently turned off and the same spot irradiated for the same time as (1). The final core-level spectra were recorded by moving from the sample, restarting the neutraliser, and returning under computer control, to the same analysis position for acquisition.
3. To study the effect of the neutraliser, the same protocol as in (2) was used, except the X-ray source was turned off following acquisition of the initial set of core-level spectra.

PDDA 20 wt% in water (M_W 200,000–350,000) was purchased from Sigma-Aldrich. Samples were prepared by drop casting on to a Si wafer which has been cleaned ultrasonically in iso-propyl alcohol. The PDDA was allowed to dry at 50 °C on a hot plate. Samples were also prepared by drop casting and drying under vacuum and leaving exposed to the lab atmosphere overnight, no difference was found between these film compositions in the XPS study.

Data was analysed using CasaXPS v2.3.24 (Fairley et al., 2021) using Scofield sensitivity factors (Scofield, 1976) and a TPP-2M electron correction (Tanuma et al., 1994) after subtraction of a Shirley type background. All peak fits are made using the Lorentzian Asymmetric (LA) lineshape in CasaXPS, which is a numerical convolution of a Lorentzian with a Gaussian to produce a lineshape based on a Voigt function. Here, LA(1.3, 243) was derived from the first N 1s spectrum recorded and found to be adequately define N 1s and C 1s species. All XPS data is presented with the lowest C 1s peak taken to be 285.0 eV and binding energies are presented with an uncertainty of ±0.2 eV.

The ^{13}C NMR spectroscopy was performed on a Bruker Ascend 400 (400 MHz), which operated at 100.61 MHz for ^{13}C nuclei. Chemical shifts are reported in parts per million (ppm).

3. Results and discussion

The structure of PDDA is shown in Fig. 1. The synthesis process involves a cyclopolymerisation process and several configurations of the resulting polymer are likely to form (Hahn and Jaeger, 1992). Previous work has shown that the polyelectrolyte consists of three isomeric forms made up of *cis* and *trans* isomers of pyrrolidinium rings, in addition to an unsaturated species containing a pendant double bond (Fig. 1) (Dautzenberg et al., 1998). The only known study of PDDA as distinct reagent previously reported that these three forms do not display resolvable differences in their N 1s binding energies due to the very similar quaternary ammonium chemical environments in each case (Yang et al., 2005). Therefore any potential change in speciation of the PDDA polymer can readily be followed using changes in the N 1s peak position.

Table 1 shows the elemental composition (at%) of the PDDA film, acquired as protocol (1) in the experimental section, where T_0 equates to the initial spectra acquired in under 5 min and T_{70} refers to the final spectra acquired after 70 min of acquisition time. The survey spectra associated with these intervals are provided in Figure S1. The results for T_0 show that the films were predominantly comprised of carbon, nitrogen and chlorine as expected, whilst oxygen, sodium and sulfur were also found.

Fitting of the C 1s spectrum reveals two peaks at 285.0 and 286.1 eV, corresponding to the sp^3 carbons β to the quaternary ammonium group, and the carbons directly bound to the ammonium group within the polyelectrolyte, respectively (Figure S2) (Yang et al., 2005). In contrast to the previously reported analysis by Sacher and co-workers, a shake-up peak (*ca.* 291 eV) was not observed within the C 1s spectrum of PDDA (Yang et al., 2005). Such shake-up structure is associated with $\pi \rightarrow \pi^*$ transitions resulting from the unsaturated species shown in Fig. 1. Whilst this species has been detected in our PDDA through $^{13}C\{^1H\}$ NMR experiments as two minor signals at 128.6 and 123.9 ppm, corresponding to the sp^2 carbon environments (see Figure S9), its absence in our films, regardless of preparation method, is attributed to the low concentration of this species within the three-component PDDA source coupled with the preferential accumulation of *cis* and *trans* isomers within the information depth of the XPS analysis (*ca.* 10 nm for C 1s).

In respect of the other elements, chlorine is observed in two states (Figure S3). The Cl $2p_{3/2}$ signal at 196.9 eV is attributed to the chloride (Cl^-) counter ion associated with the quaternary ammonium centre of PDDA (Beamson and Briggs, 1992). The second species, at 198.8 eV, is attributed to NaCl, from the PDDA source (Moeez et al., 2019). The oxygen (Figure S4), is unexpected given the structure of PDDA and with the absence of Si 2p signal of the substrate, then a signal due to any native oxide film of the Si wafer support can be discounted. Therefore its origin is likely to correspond to the presence of ^-OH, which has undergone anion exchange in aqueous solution with the Cl^- (Yang et al., 2005). Although not fitted, other than to remove the Na Auger component, there is some asymmetry to the O 1s signal, which we believe to be associated with the sulfur given the presence of sulfate and sulfite signals (Figure S5). The sodium is in too great a concentration to be associated wholly with the chlorine as discussed earlier, and therefore given the identical binding energy of Na 1s in NaCl, Na_2SO_3 and Na_2SO_4 we attribute the extra sodium (binding energy 1071.7 eV, Figure S6) to these sodium salts. The presence of Na and S are believed to come from stabilising agents in the PDDA source.

For the PDDA polymer, the expected C:N:Cl ratio is 8:1:1. Based on our data, the films give an approximate ratio of 10:1:1 (Table 1). This difference is attributed to small levels of surface contamination from the formation of the films or through some organic termination of the polymer chain.

Table 1 shows subtle differences in the T_0 and T_{70} atomic concentrations. The values and spectra associated with oxygen, sodium and sulfur remain unchanged with little deviation from the respective at% of the various environments and their binding energy values.

However, significant changes were observed in the nitrogen and carbon environments. The initial XPS analysis (T_0) of the N 1s spectrum of PDDA reveals a single nitrogen environment (402.3 eV, Fig. 2(a)) which is attributed to the quaternary ammonium group and corresponds to 100% of the total nitrogen content. For the T_{70} analysis, the content of this species reduced to 70% and two, lower binding energy species at 400.2 and 399.1 eV are found, contributing to the remaining 30% (Table 2). The lower energy species correspond to the reduction of the

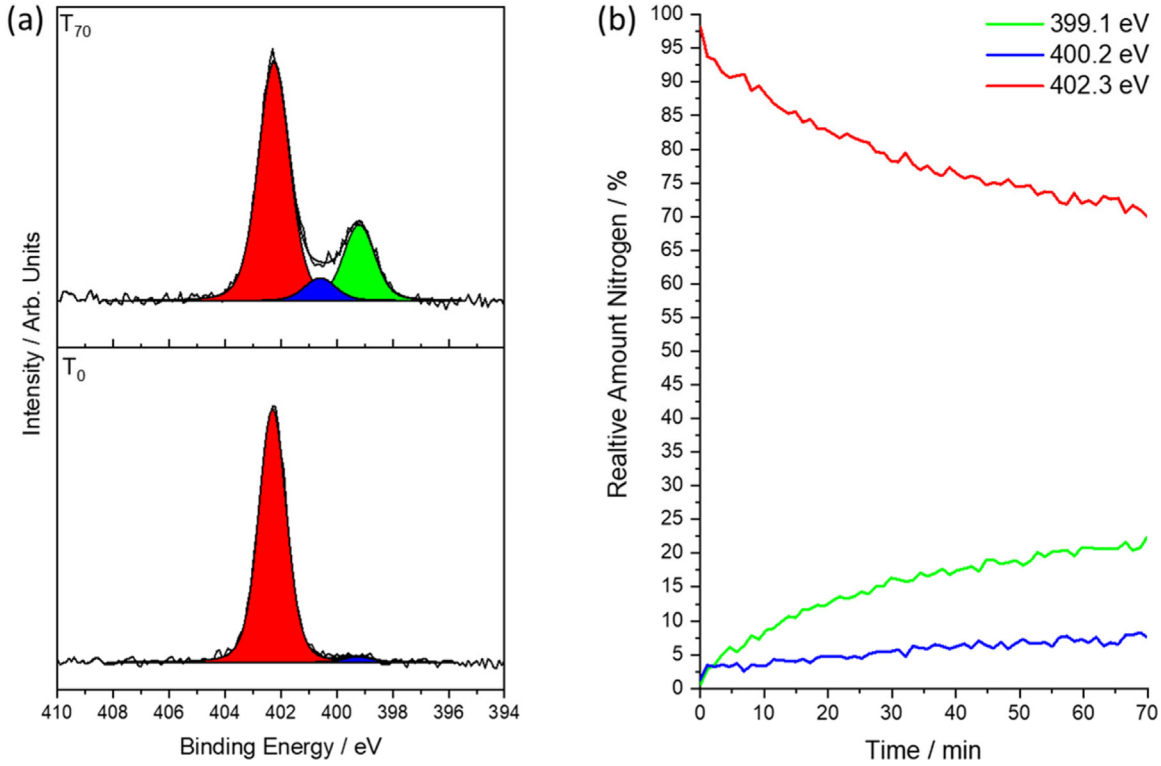

Fig. 2. (a) High-resolution N 1s spectra of PDDA acquired at 0 min (T_0, bottom) and 70 min (T_{70}, top), (b) plot of the relative at% of the N 1s peaks corresponding to the quaternary ammonium species (402.3 eV) and the reduced species (400.2 and 399.1 eV) over the 70-min time period.

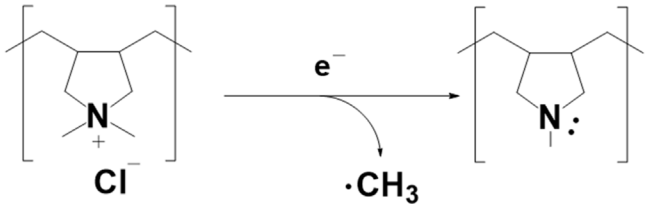

Scheme 1. Proposed mechanism for the formation of the reduced species of PDDA from the quaternary ammonium nitrogen.

Table 2
Quantitative elemental data for N 1s environments of PDDA acquired at 0 min (T_0) and 70 min (T_{70}).

Time	Relative percentage (%) of the N 1s binding energies (eV) for specified analysis method								
	X rays only			Neutraliser only			X-rays and neutraliser		
	399.1	400.2	402.3	399.1	400.2	402.3	399.1	400.2	402.3
T_0	3.1	1.90	95.0	0.0	1.20	98.9	0.0	0.50	99.5
T_{70}	14.6	7.40	78.0	14.0	5.50	80.3	22.5	7.50	70.0

quaternary nitrogen and typically, N 1s values in the range *ca.* 399 and 400 eV, are attributable to amine-like functions and consistent with previous assignments of "uncharged side products" associated with the quaternary ammonium groups (Yang et al., 2005; Wang et al., 2011; Marinoiu et al., 2020; Dong et al., 2016). Meanwhile, Marinoiu and co-workers suggest that the signal originates from PDDA partially loosing Cl^- (Marinoiu et al., 2020).

Our data suggests that the quaternary ammonium nitrogen undergoes reduction during the analysis itself, and to the best of our knowledge, no published report has presented a systematic, time-resolved study of the reduction for this polyelectrolyte.

To confirm this, we analysed the relative at% of N 1s peaks acquired across the 70-min period in more detail (Fig. 2(b)). It was found that the atomic composition of the lower binding energy species proportionately increased over this period, at the expense of the ammonium group. As evident by the respective gradients in the plot of relative concentrations in Fig. 2(b), the rate of reduction is greater in the first 20 min, after which there is a gradual plateau, signifying some limit to the extent of reduction. Clearly, depending on the analysis time frame and the experimental acquisition protocol used (such as the default programmable flow chart used by the software for acquisition) could lead analysts to believe that PDDA consists of two environments.

The change in N 1s chemistry is mirrored by changes to the C 1s spectrum (Figure S2). Whilst the initial (T_0) analysis reveals carbon environments in a 1:1 ratio, at T_{70}, the concentration of the species at 285.0 eV increases, whist the peak related to the carbon associated with the quaternary nitrogen at 286.1 eV decreases. A small decrease in the Cl 2p species at 196.9 eV suggests a loss of Cl^- associated with the quaternary ammonium nitrogen (Figure S3). A likely route for this reduction is shown in Scheme 1, whereby a methyl radical is eliminated from the species generating the tertiary amine.

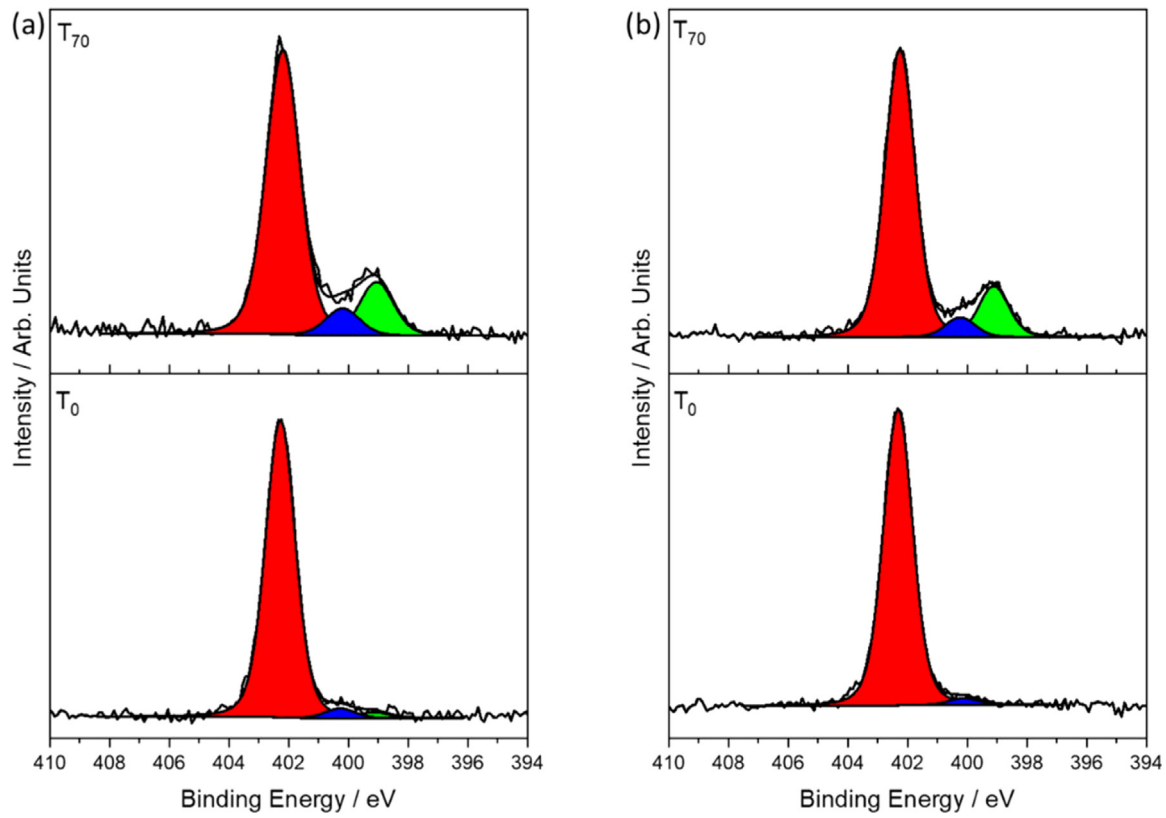

Fig. 3. High-resolution N 1s spectra of PDDA., where(a) analysed before (T_0, bottom) and after (T_{70}, top) prolonged X-ray exposure) and (b) analysed before (T_0, bottom) and after (T_{70}, top) prolonged neutraliser exposure. The colours are the same for those in Fig. 2. (For interpretation of the references to colour in this figure legend, the reader is referred to the web version of this article.)

Although the data shows the degree of reduction is related to the analysis time, the primary cause of the reduction process is not so evident. As shown by one of the present authors, degradation can occur due to X-ray irradiation itself (and damage by the subsequent secondary electron cascade) or the neutraliser (Edwards et al., 2019). An understanding of which is the major cause of damage can therefore tailor analysis of such materials. To study this further, the iterative collection of the N 1s spectrum was acquired under two different conditions, as described in the experimental section.

For the area irradiated by the X-rays, only the T_{70} spectrum (Fig. 3(a)) shows the increase of the tertiary amine signals, which account for approximately 22% of the total N 1s concentration. Repeating this analysis on a fresh area of the sample, with prolonged neutraliser-only irradiation, reveals the reduced species account for 19.5% of the total N 1s concentration. This value is not dissimilar to that of the X-ray alone. Comparison of this data with that in Fig. 2, however, shows that both X-ray and neutraliser irradiation appear to have a somewhat additive effect on the extent of reduction.

Whilst no comparative study has been made herein, using an electron only neutraliser or the use of a broad-spot monochromatic X-ray source, it is evident from the information presented that care must be taken in analysing such polymeric materials using dual charge compensation. Given the increasing popularity of compact, easy to use XPS systems, such as the K-Alpha$^+$ system employed in this study, due-care must be given to the experimental planning, together with the analyst actively investigating any unexpected spectral features and refining their experimental protocol. Scheme 2 shows an example experimental flow chart which would be akin to the default from the Thermo Avantage control software (Scheme 2(a)), together with an example of a modified flow-chart (Scheme 2(b)) to investigate the reduction in PDDA. The modified scheme assumes an initial survey

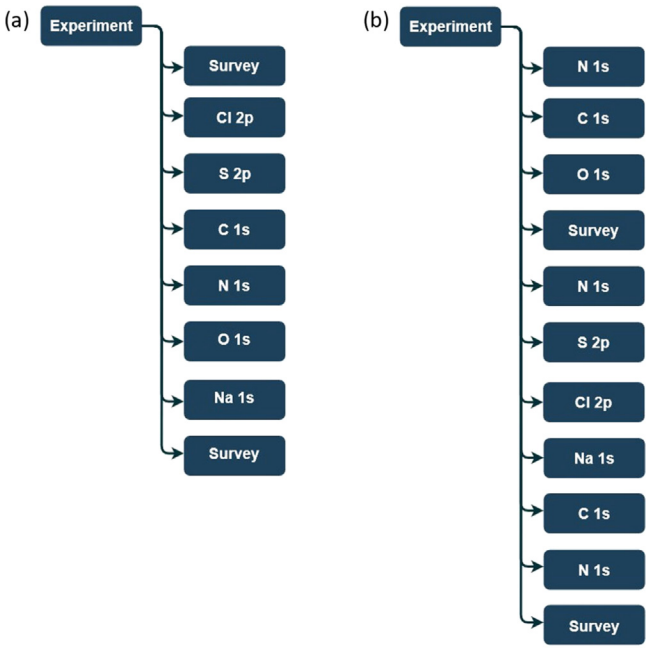

Scheme 2. Example experimental flow charts for analysis of PDDA, where (a) is an example of the default, automatically created flow chart in the acquisition software and (b) is a modified flow chart to assess any analysis induced reduction of the N 1s and C 1s regions.

and high-resolution set of spectra have been recorded and reduction assumed by the analyst and that a fresh area of the sample is now to be analysed.

For XPS data systems where the spectra are recorded concurrently, then the flow chart in Scheme 2(b) would also be appropriate.

4. Conclusions

We have shown that XPS analysis of PDDA can induce chemical alterations to its structure where the quaternary ammonium species undergoes reduction to form a tertiary amine functionality, likely through loss of a methyl radical. Changes to both N 1s and C 1s spectra support this view, with the emergence of a low binding energy N 1s species mirroring the decline of the quaternary ammonium peak. These results highlight the importance in recognising destructive effects from the analysis. For PDDA and similar materials, it is therefore recommended to analyse the N 1s and C1s spectra first and as quickly as possible, whilst periodically checking for spectra changes.

CRediT authorship contribution statement

Rachel L. McLaren: Conceptualization, Data curation, Software, Analysis, Writing – original draft, Writing – review & editing. **Gareth R. Owen:** Writing – review & editing. **David J. Morgan:** Conceptualization, Data curation, Software, Analysis, Writing – review & editing.

Declaration of competing interest

The authors declare that they have no known competing financial interests or personal relationships that could have appeared to influence the work reported in this paper.

Acknowledgements

This work was funded by European Social Fund (ESF) via the Welsh Government through a KESS2 Ph.D. studentship for R. L. M. XPS data collection was performed at the EPSRC National Facility for XPS ('HarwellXPS'), operated by Cardiff University and UCL, under contract No. PR16195.

Appendix A. Supplementary data

Supplementary material related to this article can be found online at https://doi.org/10.1016/j.rsurfi.2021.100032.

References

Baer, D.R., Engelhard, M.H., Lea, A.S., 2003a. Surf. Sci. Spectra 10, 47–56.
Baer, D.R., Gaspar, D.J., Engelhard, M.H., Lea, A.S., 2003b. Surface Analysis by Auger and X-Ray Photoelectron Spectroscopy. IM Publications.
Beamson, G., Briggs, D., 1992. In: Beamson, G., Briggs, D. (Eds.), High Resolution XPS of Organic Polymers: The Scienta ESCA300 Database. Wiley-Blackwell.
Cazaux, J., 1999. J. Electron Spectrosc. Relat. Phenom. 105, 155–185.
Cazaux, J., 2000. J. Electron Spectrosc. Relat. Phenom. 113, 15–33.
Crist, B.V., 2000. Handbook of Monochromatic XPS Spectra: Polymers and Polymers Damaged by X-Rays. Wiley & Sons, Chichester.
Dautzenberg, H., Görnitz, E., Jaeger, W., 1998. Macromol. Chem. Phys. 199, 1561–1571.
Dong, L., Zhang, X., Ren, S., Lei, T., Sun, X., Qi, Y., Wu, Q., 2016. RSC Adv. 6, 6436–6442.
Edwards, L., Mack, P., Morgan, D.J., 2019. Surf. Interface Anal. 51, 925–933.
Fairley, N., Fernandez, V., Richard-Plouet, M., Guillot-Deudon, C., Walton, J., Smith, E., Flahaut, D., Greiner, M., Biesinger, M., Tougaard, S., Morgan, D., Baltrusaitis, J., 2021. Appl. Surf. Sci. Adv. 5, 100112.
Frydman, E., Cohen, H., Maoz, R., Sagiv, J., 1997. Langmuir 13, 5089–5106.
Greczynski, G., Hultman, L., 2021. Appl. Surf. Sci. 542, 148599.
Hahn, M., Jaeger, W., 1992. Die Angew. Makromol. Chem. 198, 165–178.
Heister, K., Zharnikov, M., Grunze, M., Johansson, L.S.O., Ulman, A., 2001. Langmuir 17, 8–11.
Kam, S., Gregory, J., 1999. Colloids Surf. A 159, 165–179.
La, Y.H., Kim, H.J., Maeng, I.S., Jung, Y.J., Park, J.W., Kang, T.H., Kim, K.J., Ihm, K., Kim, B., 2002a. Langmuir 18, 301–303.
La, Y., Kim, H.J., Maeng, I.S., Jung, Y.J., Park, J.W., Kim, K.-J., Kang, T., Kim, B., 2002b. Langmuir 18, 2430–2433.
Laibinis, P.E., Graham, R.L., Biebuyck, H.A., Whitesides, G.M., 1991. Science 254, 981–983.
Marinoiu, A., Raceanu, M., Andrulevicius, M., Tamuleviciene, A., Tamulevicius, T., Nica, S., Bala, D., Varlam, M., 2020. Arab. J. Chem. 13, 3585–3600.
McLaren, R.L., da Costa, R.C., Laycock, C.J., Morgan, D.J., Warwick, M.E.A., Owen, G.R., 2021a. New J. Chem. 45, 19210–19214.
McLaren, R.L., Laycock, C.J., Brousseau, E., Owen, G.R., 2021b. New J. Chem. 45, 12071–12080.
McLaren, R.L., Laycock, C.J., Morgan, D.J., Owen, G.R., 2020. New J. Chem. 44, 19144–19154.
Mendes, P., Belloni, M., Ashworth, M., Hardy, C., Nikitin, K., Fitzmaurice, D., Critchley, K., Evans, S., Preece, J., 2003. ChemPhysChem 4, 884–889.
Moeez, I., Lim, H.-D., Park, J.-H., Jung, H.-G., Chung, K.Y., 2019. ACS Energy Lett. 4, 2060–2068.
Moon, J.H., Kim, K.-J., Kang, T.-H., Kim, B., Kang, H., Park, J.W., 1998. Langmuir 14, 5673–5675.
Rieke, P.C., Baer, D.R., Fryxell, G.E., Engelhard, M.H., Porter, M.S., 1993. J. Vac. Sci. Technol. A 11, 2292–2297.
Scofield, J.H., 1976. J. Electron Spectrosc. Relat. Phenom. 8, 129–137.
Stevie, F.A., Donley, C.L., 2020. J. Vac. Sci. Technol. A 38, 063204.
Tanuma, S., Powell, C.J., Penn, D.R., 1994. Surf. Interface Anal. 21, 165–176.
Wagner, A.J., Han, K., Vaught, A.L., Fairbrother, D.H., 2000. J. Phys. Chem. B 104, 3291–3297.
Wang, S., Wang, X., Jiang, S.P., 2011. Phys. Chem. Chem. Phys. 13, 6883.
Yang, D., Rochette, J., Sacher, E., 2005. J. Phys. Chem. B 62, 4481–4484.
Zharnikov, M., Grunze, M., 2002. J. Vac. Sci. Technol. B 20, 1793.